Dear Reviewer,

We thank you for reviewing our paper and giving us encouraging comments. We took all your comments into consideration, particularly in clarifying the initial molar concentrations of all simulations.

Below we provide the point-by-point responses. All modifications of the manuscript have been highlighted in red.

Sincerely,
Po-Wei Huang
powei.huang@erdw.ethz.ch
Postdoctoral Researcher, Geothermal Energy and Geofluids Group,
Institute of Geophysics, ETH Zurich

Reviewer's comments

Comment 1 — In Figure 1, a flow chart is represented. I suggest to use the same notation for the velocity as in the text of the manuscript.

Reply: Thank you for pointing out the inconsistent notation in the flow chart. Throughout the manuscript, we used $\boldsymbol{u}$ as the notation for the barycentric velocity. However, in Figure 1, we used $\vec{v}$ to represent the barycentric velocity. We corrected the flow chart. Please refer to the excerpts below.

Figure 1. Flow chart of the simulation procedures

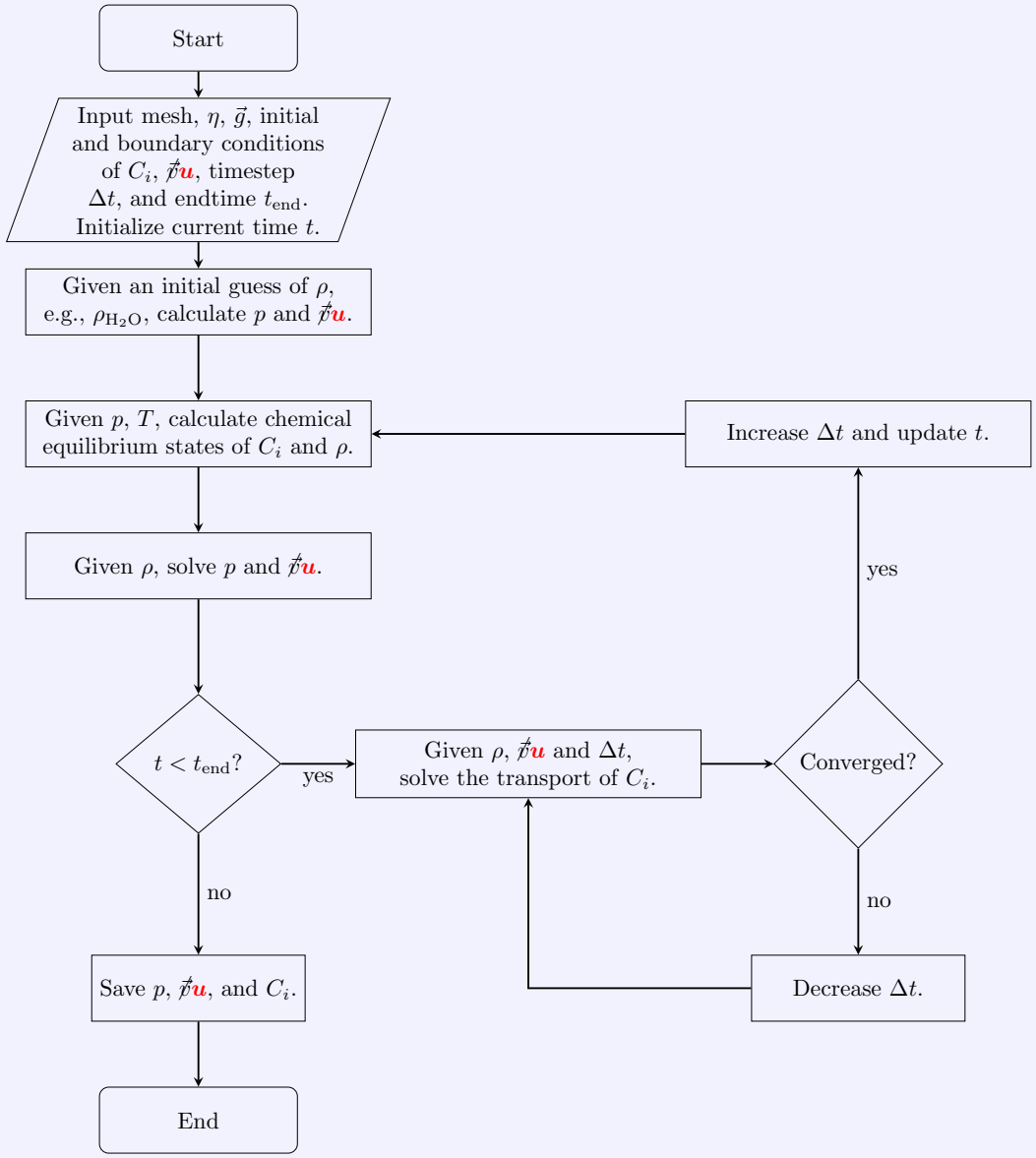

Comment 2 — Since the Nernst–Planck equation is non-stationary, for the sake of clarity, I suggest that you write the equation from which initial molar concentrations are obtained, to make everything mathematically more clearly, since for the boundary conditions no-flow boundary conditions are taken, the initial conditions must be written clearly.

Reply: We clarify the initial conditions of the mass transport equations by adding Table 3 to Section 2.3. Whenever the setup of the simulations is discussed in the text, we add a sentence that refers to Table 3 to ensure the initial conditions are clarified. The table is miniaturized to fit in the excerpts below. Please refer to the corrected manuscript for the full-sized table.

2.3 Selected experiments for model evaluation

No-flow boundary conditions are prescribed on all sides of the simulation domain. Table 3 specifies the chemical compositions of the aqueous solutions, which defines the initial conditions of the mass transport equations.

Table 3. The chemical compositions of the aqueous solutions. The unit of the chemical compositions is in $\mathrm{mol\,L^{-1}}$. In the table, dashes denote "not applicable" because the chemical species are not considered in the simulation cases.

	H^+	OH^-	Na^+	Cl^-	Li^+	$NO_3{}^-$	$HCO_3{}^-$	$CO_3{}^{2-}$	$CO_2(aq)$	$H_2O(l)$
1M HCl	1.0	2.109×10^{-14}	10^{-20}	1.0	-	-	-	-	-	54.170
1M NaOH	2.199×10^{-14}	1.0	1.0	10^{-20}	-	-	-	-	-	55.360
1.4M NaOH	1.537×10^{-14}	1.4	1.4	-	-	10^{-20}	-	-	-	55.361
1.5M HNO_3	1.5	1.287×10^{-14}	10^{-20}	-	-	1.5	-	-	-	52.712
0.01 M LiOH	1.235×10^{-12}	0.01	-	-	0.01	-	10^{-20}	10^{-20}	10^{-20}	55.345

2.3.1 Chemically driven convection of acid–base systems

Please refer to the left panel of Figure 2 for the setup. Table 3 lists the chemical composition of 1 M HCl and 1 M NaOH. The prescribed minimum timestep size is 3×10^{-2} seconds, and the maximum timestep size is 2.0 seconds.

...

The setup is shown in Figure 2, and Table 3 lists the initial chemical composition of 1.5 M HNO_3 and 1.4 M NaOH. The prescribed minimum timestep size is 1×10^{-3} seconds, and the maximum timestep size is 1.0 seconds.

2.3.2 Convective dissolution of CO2 in reactive alkaline solutions

We consider the following species as the main fluid components in the case of convective dissolution of CO_2: H^+, OH^-, Li^+, $CO_2(aq)$, $HCO_3{}^-$, $CO_3{}^{2-}$, and $H_2O(l)$, and the initial conditions are presented in Table 3. The prescribed minimum and maximum timestep sizes are 5×10^{-3} seconds and 1.5 seconds, respectively.

Comment 3 — Could you please elaborate, how large is the system in (32) when you update the velocity, and explain the reason why you have chosen to solve it with direct solver? (Just to comment: since you have used direct solver for linear system (in which possibly positive-definite matrix is added (rB^TB)) maybe you could try to use some iterative solver from PETSc, the library that was also used in this work for resolving nolinearity in transport equation)

Reply: Since we use the Raviart–Thomas basis for the velocity, the number of degree of freedom is the same as the number of cell faces (edges for 2D meshes). For the simulation cases (HCl–NaOH, HNO_3–NaOH, CO_2 dissolution), the edge counts are 52053, 17464, and 138576, respectively. We added the range of degrees of freedom into the manuscript.

We tried to use iterative solvers such as PETSc to calculate the first iteration of the augmented Lagrangian Uzawa's method, Eq. (32). We encountered convergence issues and could not find a suitable algebraic preconditioner to achieve convergence. This is why we calculate Eq. (32) by a direct solver.

To elaborate on why we did not calculate Eq. (32) by an iterative solver, we referenced Fortin and Glowinski, 1983 in Section 2.2.1 to motivate the use of direct solvers. Please refer to the excerpts below.

2.2.1 The barycentric flux

However, the matrix $A + rB^TB$ becomes more ill-conditioned as r increases, which may lead to a large number of iterations to solve when applying an iterative method (Fortin and Glowinski, 1983). Hence, we use the MUMPS (Amestoy et al., 2001; Amestoy et al., 2019) direct solver to update the velocity, Eq. (32). The degrees of freedom of $\boldsymbol{u}$ in our simulations range from 17 000 to 140 000.

Comment 4 — Could you please elaborate the stepsizes Δt that have used in your simulations?

Reply: We added descriptions of the adaptive timestep sizes in Section 2.2.2. Furthermore, we added detailed timestep sizes Δt we used in the simulations in Sections 2.3.1 and 2.3.2. Please refer to the excerpts below and the excerpts in Comment 2.

2.2.2 Transport of fluid components

With regard to the time-stepping schemes, we use an explicit scheme for the upwind advection term and the Crank–Nicolson scheme for the diffusion and Nernst–Planck terms. The timestep size Δt is determined in an adaptive manner, where the minimum and maximum timestep sizes are prescribed for each simulation.

References

Amestoy, P. R. et al. (2001). "A Fully Asynchronous Multifrontal Solver Using Distributed Dynamic Scheduling". In: *SIAM J. Matrix Anal. A.* 23.1, pp. 15–41. DOI: 10.1137/S0895479899358194.

Amestoy, P. R. et al. (2019). "Performance and Scalability of the Block Low-Rank Multifrontal Factorization on Multicore Architectures". In: *ACM T. Math. Software* 45 (1), pp. 1–26. DOI: 10.1145/3242094.

Fortin, M. and R. Glowinski (1983). "Augmented Lagrangian Methods in Quadratic Programming". In: *Augmented Lagrangian Methods: Applications to the Numerical Solution of Boundary-Value Problems*. Ed. by Michel Fortin and Roland Glowinski. Vol. 15. Studies in Mathematics and Its Applications. Elsevier. Chap. 1, pp. 1–46. DOI: 10.1016/S0168-2024(08)70026-2.